Quantum mechanical effects in the silicon quantum dot in a single-electron transistor

Hiroki Ishikuro[a] and Toshiro Hiramoto[b]
Institute of Industrial Science, University of Tokyo, 7-22-1 Roppongi, Minato-ku, Tokyo 106, Japan

(Received 17 July 1997; accepted for publication 23 October 1997)

The quantum mechanical effects in silicon single-electron transistors have been investigated. The devices have been fabricated in the form of point contact metal–oxide–semiconductor field-effect transistors with various channel widths using electron beam lithography and the anisotropic etching technique on silicon-on-insulator substrates. The device with an extremely narrow channel shows Coulomb blockade oscillations at room temperature. At low temperatures, negative differential conductances and fine structures are superposed on the device characteristics, which are attributed to the quantum mechanical effects in the silicon quantum dot in the channel. The energy spectrum of the dot is extracted from the experimental results. © *1997 American Institute of Physics.* [S0003-6951(97)02951-3]

The operating temperature of single-electron devices[1] depends on the dot size in the devices. Many attempts have been made previously to fabricate small dots in order to raise the temperature of the device operations. Since silicon single-electron devices operating at room temperature[2–5] require an ultrasmall Si dot whose size is typically less than 10 nm, the role of quantum mechanical effects such as discrete energy levels in the dots[6,7] or the fluctuation of the density of states in source and drain region[8] cannot be ignored and will have a significant influence on the device characteristics. It is more important to understand the quantum mechanical effects on device characteristics as the device size decreases.

In this work, quantum mechanical effects in silicon single-electron transistors have been investigated. The devices have been fabricated in the form of point contact metal–oxide–semiconductor field-effect transistors (MOSFETs) using electron beam (EB) lithography and the anisotropic etching technique. Coulomb blockade oscillations are seen at room temperature in devices with extremely narrow channels. At low temperatures, negative differential conductances (NDCs) and fine structures are superposed on the device characteristics. We have estimated the electronic structure of the quantum dot in a channel from the gate voltage and drain voltage dependence of the drain current.

Figure 1 shows the schematic view of the point contact MOSFET. A (001) oriented, p-type silicon-on-insulator (SOI) substrate prepared by the separation by implanted oxygen (SIMOX) technique is employed. The point contact channel is defined by the EB lithography. The anisotropic etching technique is employed to compensate the fluctuations caused by the EB lithography.[9] Tetramethylammonium-hydroxide which is fully compatible with the current very large scale integrated (VLSI) process[4,5,10] is utilized for anisotropic etching. The thickness of the SOI layer is less than 20 nm and the gate oxide at (001) surface is 50 nm. The channel width is changed by changing the electron dose of the EB lithography.

The characteristics of the point contact MOSFET strongly depend on the channel width. The device with a large width has the normal MOSFET characteristics. By scanning electron microscopy observation, we have found that the device with 30 nm width shows normal MOSFET operation even at 4.2 K. As the width decreases, the drain current decreases and, when the channel is extremely narrow, the device shows clear Coulomb blockade oscillations, which indicates that the channel is separated by tunnel barriers. When the width further decreases, the device has no drain current because the channel is cut off by the thermal oxidation.

The reason why the channel is separated into dots is not clear at present and is under investigation. The thickness fluctuations[2] of the SOI layer would not be the cause of the dot formation because the period of the thickness fluctuations in SIMOX is much larger than the channel length of the device. The localized states or Si nanoparticles at the interface between the SOI layer and the buried oxide layer, or pattern dependent oxidation[3] may turn out to be the reason for the dot formation.

Figure 2 shows the drain current as a function of V_g in a device which shows Coulomb blockade oscillations even at room temperature. It should be noted that the intervals between the peaks are not constant. Figure 3 shows the V_{ds}

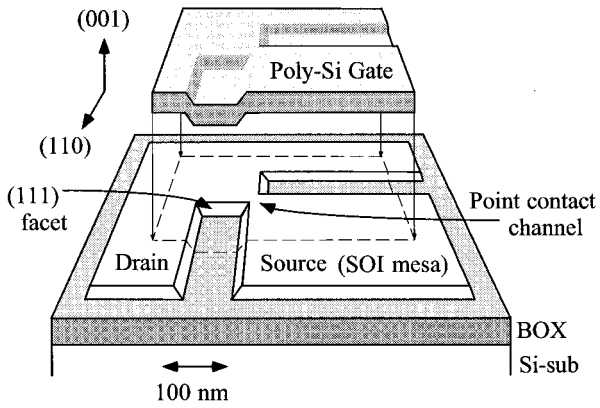

FIG. 1. Schematic view of the Si point contact MOSFET.

[a]Electronic mail: ishikuro@nano.iis.u-tokyo.ac.jp
[b]Also at the VLSI Design and Education Center, University of Tokyo, 7-3-1 Hongo, Bunkyo-ku, Tokyo 113, Japan.

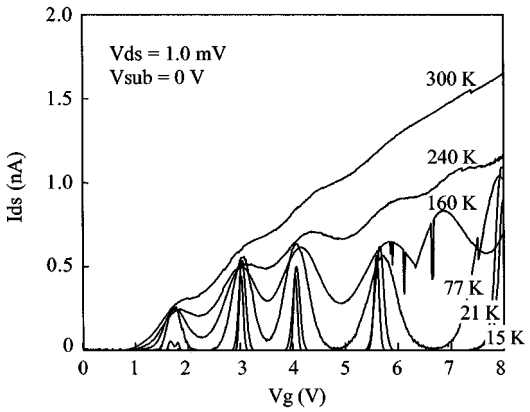

FIG. 2. Dependence of the drain current (I_{ds}) on gate voltage (V_g) with a drain voltage (V_{ds}) of 1.0 mV. The temperature is changed from room temperature down to 21 K. The abrupt I_{ds} changes at 160 K are the random telegraph noise.

dependence of the I_{ds} near the Coulomb blockade oscillation peak (at $V_g = 3.9$ V). The NDCs (at $V_{ds} \simeq \pm 100$ meV) and fine structures (at $V_{ds} \simeq +40, -50$ meV) are clearly observed as well as the I_{ds} region suppressed by Coulomb blockade at low drain voltage ($|V_{ds}| < 10$ meV). To grasp the entire property of the device, we took the I_{ds} dependence on the V_{ds} and V_g in Fig. 4. Clear rhombus shapes which are caused by the Coulomb blockade are observed. Furthermore, the NDCs and fine structures appear in parallel with the sides of the rhombus shapes. Then, we consider the transport properties of the channel in what follows.

In Fig. 2, the temperature dependence of the peak heights is not strong and the peaks do not split at low temperature as in the case of multiple-dot system.[5,11,12] In Fig. 4, where the V_g is fixed at oscillation peaks, the rhombus shapes of the current suppressed regions are closed and the $I_{ds} - V_{ds}$ characteristics are perfectly linear at low V_{ds}. Therefore, the Coulomb blockade effects are caused by a single-dot system.

Different from the Coulomb blockade characteristics of the semi-classical model,[1] (i) the interval between the oscillations peaks is not constant (Fig. 2) and (ii) NDCs and the

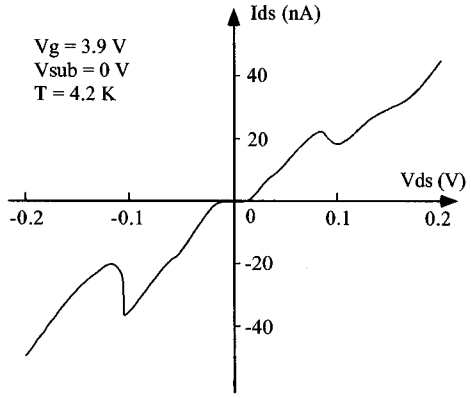

FIG. 3. $I_{ds} - V_{ds}$ characteristics near the Coulomb blockade oscillation peak at 4.2 K. NDCs are observed at $V_{ds} \simeq \pm 100$ meV and fine structures appear at $V_{ds} \simeq +40, -50$ meV.

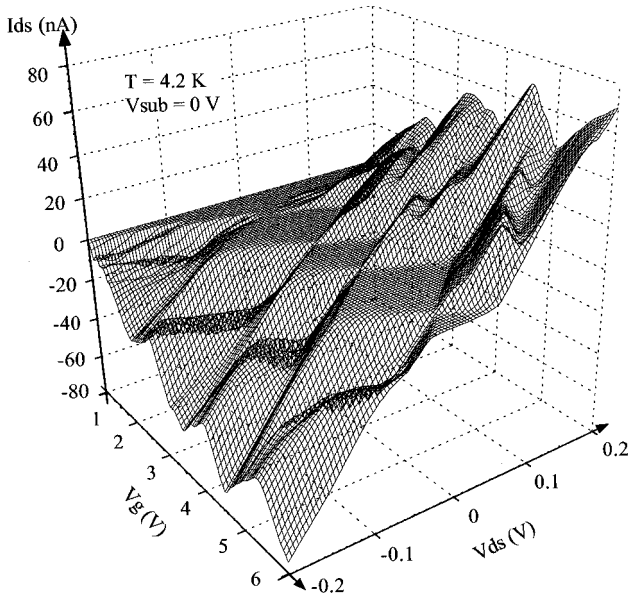

FIG. 4. Three-dimensional plot of the I_{ds} as a function of the V_g and V_{ds} at 4.2 K. Clear rhombus shapes caused by Coulomb blockade oscillations are observed. NDCs and fine structures appear in parallel with the sides of the rhombus shapes.

fine structures are superposed on the $I_{ds} - V_{ds}$ characteristics (Figs. 3 and 4).

We attribute the cause of the anomalous characteristics to the quantum mechanical effects. In a small semiconductor dot, the separations between the single-electron energy levels become comparable to the single-electron charging energy, which breaks the periodicity of the Coulomb blockade oscillations.[1] NDCs would be observed when the conduction band edge of the source passes by the ground state level of the dot. On the other hand, fine structures should be observed when the Fermi level of the source corresponds to the excited state level of the dot.[6,7] Then, we could estimate the electronic structure in the dot. Each peak position of the $I_{ds} - V_g$ characteristics corresponds to the ground state energy in the dot. On the other hand, we can pick up the excited energy levels from the fine structures of the $I_{ds} - V_{ds}$ characteristics.

To extract the electronic structure in the quantum dot, we take a contour plot of the differential conductance ($\partial I_{ds}/\partial V_{ds}$) as a function of V_g and V_{ds} in Fig. 5. The hatched areas indicate the NDCs and the dotted areas represent the fine structures. From the slope of each side of the rhombus shapes ($\partial V_g/\partial V_{ds}$), we can calculate the ratio of the gate–dot (C_g), drain–dot (C_d), and source–dot (C_s) capacitance.[1] It is also possible to estimate the ratio of the substrate–dot (C_{sub}) and C_g from the shift of Coulomb blockade oscillations by the substrate bias (not shown here). In this device, the relation is estimated as $C_g : C_d : C_s : C_{\text{sub}} = 1 : 5.9 : 9.4 : 0.01$. From these values, the potential in the quantum dot (ϕ_{dot}) is changed by $\Delta\phi_{\text{dot}} = C_g \Delta V_g / C_{\text{total}} = 0.061 \Delta V_g$ when the gate voltage is changed by ΔV_g and the voltages of the other leads are fixed. In the same way, ϕ_{dot} is changed by $\Delta\phi_{\text{dot}} = C_d \Delta V_{ds} / C_{\text{total}} = 0.36 \Delta V_{ds}$ when the drain voltage is changed by ΔV_{ds} and the voltages of the other leads are fixed.

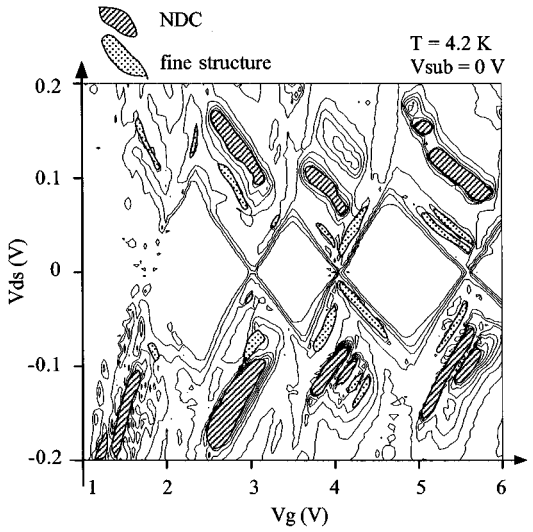

FIG. 5. Contour plot of the differential conductance ($\partial I_{ds}/\partial V_{ds}$) as a function of V_g and V_{ds} at 4.2 K. The hatched areas indicate the NDCs and the dotted areas show the fine structures. One step corresponds to 100 nS.

Using the above relations, we estimate the electronic structure in the quantum dot from Fig. 5. Figure 6 shows the corresponding energy of the ground states and excited states as a function of the number of electrons (N) in the quantum dot. The average single-electron charging energy (E_C) is 58 meV and the quantized level separation at $N=2$ is 30 meV. The barrier height of the tunnel junctions is no less than 340 meV from the gate–voltage dependence. Therefore, the sum of the charging energy and quantized level spacing in the dot as well as tunnel barrier height are much larger than the thermal energy at 300 K. Once the E_C is obtained, the average capacitances are evaluated as $C_g=0.085$, $C_d=0.50$, $C_s=0.80$, $C_{\mathrm{sub}}=0.0009$ aF. From these values, the dot size is estimated to be 6 nm if a spherical dot shape is assumed.

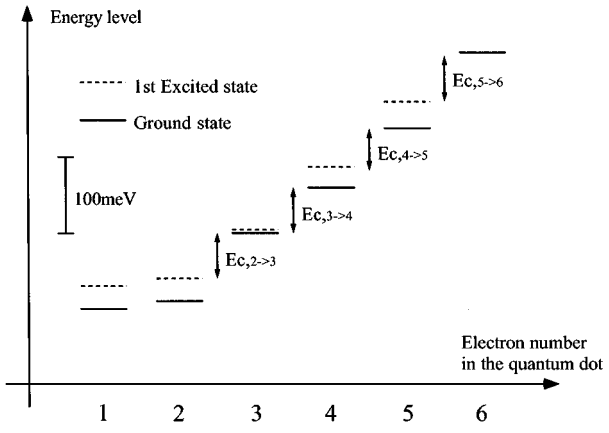

FIG. 6. Energy spectrum of N electron states in the quantum dot extracted from the fine structure of Fig. 5. The horizontal axis indicates the number of electrons and the vertical axis shows the energy levels.

The quantized level separation is strongly dependent on the number of electrons, because it is strongly affected not only by the size but also by the shape of the dot. The dot would be irregular in shape in this system. Furthermore, the quantized level separation seems to increase as the number of electrons increases which indicates that the confinement of the potential barrier of the dot is stronger than that of a harmonic potential well. On the other hand, the above mentioned capacitances and charging energy are not constant. They are also weakly dependent on the number of electrons. This is because, when the dot size and the electron number are extremely small, the charge distribution and the size of the dot are completely changed by the addition of only one electron. Therefore, the single-electron charging energy as well as the separation between the quantized levels are not constant but depend on the number of electrons in the dot.

In this device, the NDCs and fine structures are smeared out at 77 K (not shown here) and the characteristics become like a semi-classical model except for the aperiodicity of the oscillations. However, the quantum mechanical effects will become more prominent and have a significant influence on the device characteristics as the size of the quantum dots in the single electron devices decreases.

In conclusion, the quantum mechanical effects in silicon single-electron devices have been investigated. The devices have been fabricated in the form of point contact MOSFETs using the anisotropic etching technique. The device with an extremely narrow channel shows Coulomb blockade oscillations at room temperature. NDCs and fine structures are also observed at low temperatures. We have extracted the energy spectrum of the quantum dot from the transport properties of the device. The experimental results suggest that the accurate understanding of the electronic states in the dot becomes much more important for the design of extremely small single-electron devices for room temperature operation.

[1] Single Charge Tunneling, edited by H. Grabert and M. H. Devoret (Plenum, New York, 1992).
[2] K. Yano, T. Ishii, T. Hashimoto, T. Kobayashi, F. Murai, and K. Seki, IEEE Trans. Electron Devices **ED-41**, 1628 (1994).
[3] Y. Takahashi, M. Nagase, H. Namatsu, K. Kurihara, K. Iwadate, Y. Nakajima, S. Horiguchi, K. Murase, and M. Tabe, Electron. Lett. **31**, 136 (1995).
[4] T. Hiramoto, H. Ishikuro, T. Fujii, T. Saraya, G. Hashiguchi, and T. Ikoma, Physica B **227**, 95 (1996).
[5] H. Ishikuro, T. Fujii, T. Saraya, G. Hashiguchi, T. Hiramoto, and T. Ikoma, Appl. Phys. Lett. **68**, 3585 (1996).
[6] G. W. Bryant, Phys. Rev. B **39**, 3145 (1989).
[7] G. W. Bryant, Phys. Rev. B **44**, 3782 (1991).
[8] T. Schmidt, R. J. Haug, V. I. Fal'ko, K. v. Klitzing, A. Förster, and H. Lüth, Phys. Rev. Lett. **78**, 1540 (1997).
[9] H. Ishikuro and T. Hiramoto, Abstracts of the Silicon Nanoelectronics Workshop, 1997, p. 64.
[10] G. Hashiguchi and H. Mimura, Jpn. J. Appl. Phys., Part 2 **33**, L1649 (1994).
[11] G. Chen, G. Klimeck, S. Datta, G. Chen, and A. Goddard III, Phys. Rev. B **50**, 8035 (1994).
[12] F. R. Waugh, M. J. Berry, D. J. Mar, R. M. Westervelt, K. L. Champman, and A. C. Gossard, Phys. Rev. Lett. **75**, 705 (1995).